



## Microfluidic Reactor for the Electrochemical Reduction of Carbon Dioxide: The Effect of pH

Devin T. Whipple, Eryn C. Finke, and Paul J. A. Kenis<sup>\*z</sup>

Department of Chemical and Biomolecular Engineering, University of Illinois at Urbana-Champaign, Urbana, Illinois 61801, USA

This article reports the development and characterization of a microfluidic reactor for the electrochemical reduction of carbon dioxide. The use of gas diffusion electrodes enables better control of the three-phase interface where the reactions take place. Furthermore, the versatility of the microfluidic reactor enables rapid evaluation of catalysts under different operating conditions. Several catalysts as well as the effects of electrolyte pH on reactor efficiency for reduction of CO<sub>2</sub> to formic acid were tested. Operating at acidic pH resulted in a significant increase in performance: faradaic and energetic efficiencies of 89 and 45%, respectively, and current density of ~100 mA/cm<sup>2</sup>.

© 2010 The Electrochemical Society. [DOI: 10.1149/1.3456590] All rights reserved.

Manuscript submitted January 27, 2010; revised manuscript received April 7, 2010. Published June 29, 2010.

Carbon dioxide is widely regarded as one of the most significant contributors to climate change.<sup>1</sup> Concerted efforts are needed to significantly reduce carbon emissions, so the effects of climate change can be slowed down or, ideally, reverted. Numerous strategies for reducing emissions are being evaluated, including carbon capture and sequestration and increasing the use of carbon neutral power sources such as wind, solar, and nuclear.<sup>2,3</sup> However, the conversion of CO<sub>2</sub> into small organic molecules is more attractive than sequestration because it produces a valuable product, and intermittent power sources such as wind and solar would require a means of storing their energy before they could provide a large portion of our electricity. The electrochemical conversion of CO<sub>2</sub> is a particularly attractive process because it provides beneficial use for captured CO<sub>2</sub> and a renewable source of organic compounds that are typically derived from fossil fuels.<sup>2</sup> In addition, the electrochemical reduction of CO<sub>2</sub> to liquid fuels provides a convenient, high energy density means of storing renewable electricity.

Over the last several decades, various catalysts have been researched for the reduction of CO<sub>2</sub> into different products, mainly formic acid,<sup>4-7</sup> CO,<sup>6,8,9</sup> methane,<sup>10,11</sup> and methanol.<sup>12,13</sup> In addition, researchers have shown that the composition of the electrolyte can have a significant effect on the selectivity of CO<sub>2</sub> reduction on copper electrodes in both aqueous<sup>14,15</sup> and organic<sup>11</sup> media. Some studies have also included the variation of pH of the electrolyte, but these studies seem to have been limited to basic media.<sup>14,15</sup>

Recently, several reactor designs have been reported for CO<sub>2</sub> reduction to formic acid<sup>16-20</sup> and CO.<sup>9,21,22</sup> Many of these designs have been based on fuel cell designs and most use a polymer electrolyte membrane to separate the anode and cathode. The work by Li and Oloman on a continuous reactor with a cocurrent flow of CO<sub>2</sub> gas and catholyte through a three-dimensional cathode has been particularly extensive.<sup>15,18,23</sup> Previously, we reported a microfluidic H<sub>2</sub>/O<sub>2</sub> fuel cell in which the anode and cathode are separated by a flowing liquid electrolyte.<sup>24</sup> Here we report on a microfluidic reactor that is similar in design to this fuel cell for the efficient reduction of CO<sub>2</sub> to formic acid using different catalysts and different operation conditions, most notably different pH values.

### Experimental

**Electrochemical cell.**— Figure 1 shows a schematic of the reactor design that we used in this study. A 1.5 mm thick poly(methyl methacrylate) (PMMA) sheet with a 0.5 × 2 cm window was placed between two gas diffusion electrodes (GDEs). On the cathode side, the catalyst was applied only to the first 1.5 cm and a poly(tetrafluoroethylene) filter (10 μm, Pall Life Sciences) was added to cover the last 0.5 cm. This facilitated the removal of

bubbles (from oxygen evolution on the anode) that entered the electrolyte stream and could otherwise collect and block electrolyte contact with the catalyst. A graphite current collector with a window allowing the flow of gases backed each GDE. Behind the cathode, a PMMA chamber was placed for CO<sub>2</sub> to flow through while the anode was left open to air for oxygen to escape. Ten insulated bolts held the entire setup together.

**Electrode preparation.**— The electrodes were prepared as previously reported<sup>24</sup> using E-TEK “S”-type GDEs. In short, a suspension of catalyst and Nafion binder was made by sonicating with a 50/50 mixture of water and isopropyl alcohol, which was then painted on the GDE followed by hot-pressing. The cathodes consisted of either 2 or 5 mg/cm<sup>2</sup> catalyst and 0.1 mg/cm<sup>2</sup> Nafion. The anode was 2 mg/cm<sup>2</sup> Pt black with 0.1 mg/cm<sup>2</sup> Nafion. All electrodes were hot-pressed at 130°C and 2000 kPa for 5 min.

**Cell testing.**— An Autolab potentiostat (PGSTAT-30, EcoChemie) was used to control the cell potential and measure the resulting current. The individual electrode potentials were measured using multimeters connected between each electrode and a Ag/AgCl reference electrode (RE-5B, BASi) in the exit stream. The cell was allowed to reach steady state for 200 s, after which the electrolyte was collected and the current averaged for another 200 s before stepping to the next potential. All experiments were run at ambient conditions. The electrode potentials were not corrected for IR drop. A mass flow controller (32907-80, Cole Palmer) was used to flow CO<sub>2</sub> from a cylinder at 5 sccm, and a syringe pump (PHD 2000, Harvard Apparatus) supplied the electrolyte at 0.5 mL/min. The formate concentrations were analyzed using the colorimetric method reported by Sleat and Mah.<sup>25</sup> This method reacts formate with citric acid to give a strong absorbance at 510 nm, allowing quantitative determination with a spectrophotometer.

**Catalyst testing.**— The catalyst loading for each electrode was 2 mg/cm<sup>2</sup> (metals basis) for each cathode, and 0.5 M KHCO<sub>3</sub> was used as the electrolyte. Ru–Pd was chosen as a cathode catalyst because the work by Furuya et al.<sup>5</sup> showed it to have a high faradaic efficiency for formic acid and low overpotential. Ru–Pd catalyst is not commercially available so carbon-supported Ru–Pd was synthesized using two different methods from the literature,<sup>26,27</sup> resulting in catalysts with Ru–Pd wt % of 17–17 and 30–30. A commercial Sn nanopowder (Sigma-Aldrich) was used for comparison.

**Performance as a function of pH.**— Tin was used as the cathode catalyst with a loading of 5 mg/cm<sup>2</sup>. KCl of 0.5 M concentration was used as the electrolyte and was adjusted using 1 M HCl or 1 M KOH to pH 4, 7, and 10, as indicated by a pH probe (Orion 9157BNMD, Thermo Electron).

\* Electrochemical Society Active Member.

<sup>z</sup> E-mail: kenis@illinois.edu

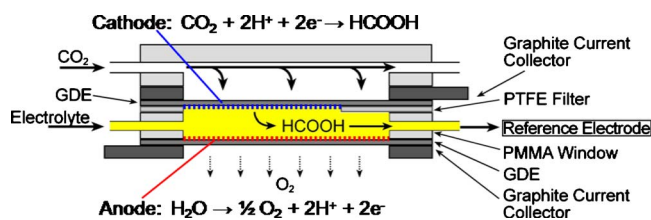


Figure 1. (Color online) Schematic diagram of the microfluidic reactor for CO<sub>2</sub> conversion.

## Results and Discussion

**Reactor design.**— In this study we use an electrochemical cell in which two GDEs are separated by a flowing electrolyte stream (Fig. 1). This microfluidic configuration is a modification of a hydrogen fuel cell that we reported previously.<sup>24,28</sup> The flowing stream provides flexibility in operation conditions, including the exact composition and pH of the electrolyte. Furthermore, any water management issues at the electrodes (flooding or dry-out) can be minimized. On the cathode side, a gaseous stream of CO<sub>2</sub> is introduced, while on the anode side, oxygen is removed. The other product, formic acid, forms at the cathode and is carried out of the reactor with the electrolyte stream. The half-cell reactions for each electrode are shown in Fig. 1. The reference electrode in the outlet of the electrolyte stream allows for an independent analysis of the processes at the individual electrodes. This microfluidic platform enables a rapid evaluation of different catalysts under different operation conditions as described below.

**Catalyst comparison.**— Figure 2a shows the current densities for the microfluidic reactor using three different cathode catalysts. As seen in the figure, the current density of Ru–Pd/C 30 wt % is the highest, followed by Ru–Pd/C 17 wt % and then Sn. However, when looking at the partial current density, which is the portion of the current that goes to the desired reaction, we see the opposite trend with the Sn catalyst having the highest performance, i.e., the highest rate of formate production.

Figure 2b compares two efficiencies, faradaic and energetic, for the three cathode catalysts. The faradaic or current efficiency, which is the most common parameter reported, is a measure of selectivity and is the portion of the current passing through the cell that goes to the desired product. In comparison, the energetic efficiency is the fraction of the energy supplied to the reactor that is contained in the product stream of the reactor. The energy in the products can be found by multiplying the free energy for the reaction of carbon dioxide and water to form formic acid and oxygen by the rate of formic acid formation. The energetic efficiency is then this value divided by the power supplied to the reactor (voltage multiplied by current). Alternatively, the energetic efficiency can be found by multiplying the faradaic efficiency by the ratio of the standard cell potential for the reactions (–1.43 V in this case) to the actual cell potential.<sup>29</sup> Both methods are equivalent and give the same result. Despite the obvious importance of the energetic efficiency, typically, only the faradaic efficiency is reported.

As seen in Fig. 2b, despite having a much higher overpotential, as indicated by the peak performance occurring at more extreme cell potentials, the Sn catalysts' faradaic and energetic efficiencies still far exceeded that of both Ru–Pd catalysts. Because of its superior performance, the Sn catalyst was used in subsequent experiments intended to investigate the effect of pH on CO<sub>2</sub> reduction efficiency.

**Comparison of performance at different pH.**— Figure 3a and b shows the partial current densities and efficiencies of the Sn catalyst in 0.5 M KCl electrolyte that has been adjusted with 1 M HCl or 1 M KOH to pH 4, 7, and 10. The data show a dual benefit of lower, more acidic pH on the reduction of CO<sub>2</sub> to formic acid. First, lowering the pH results in higher current densities for formic acid, which indicates improved reaction kinetics at lower pH. Lowering

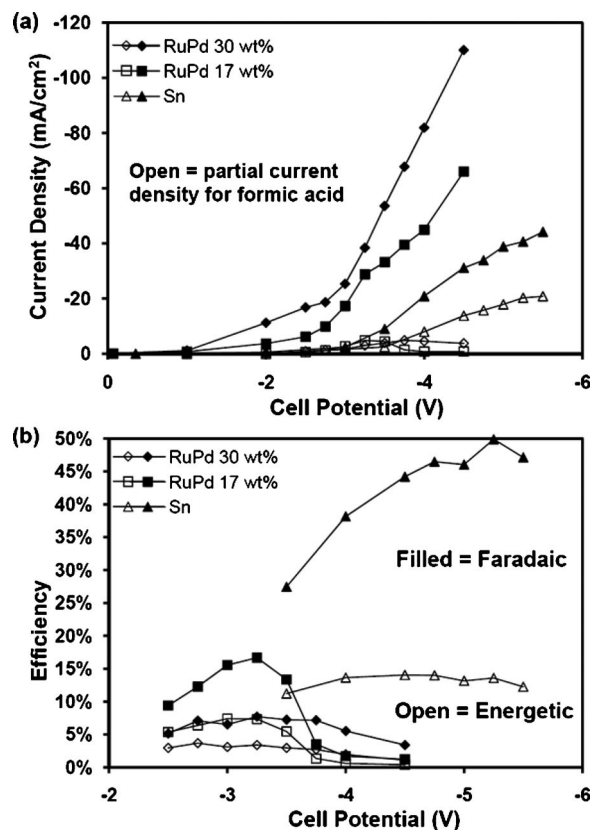


Figure 2. (a) Current densities of the reactor using three different cathode catalysts with 0.5 M KHCO<sub>3</sub> electrolyte and Pt black anode. Filled symbols indicate the total current density, with open symbols showing the partial current density for CO<sub>2</sub> reduction to formic acid, i.e., the portion of the current yielding formic acid. (b) Efficiencies using the three different cathode catalysts. Filled symbols indicate faradaic efficiency, while open symbols show the energetic efficiency.

the pH also increases the selectivity of the catalyst as indicated by the increase in faradaic efficiency. This second observation agrees with trends reported by others;<sup>15</sup> however, the earlier work was limited to basic pH and also had different ionic species, e.g., HCO<sub>3</sub><sup>–</sup> vs CO<sub>3</sub><sup>2–</sup>, at different pH. The data reported here avoid such complications and extend the range to include acidic pH. Tests were not performed at lower pH because of the instability of Sn at pH < 3.<sup>30</sup> The peak faradaic and energetic efficiencies were 89 and 45%, which are comparable to values achieved in the literature.<sup>18,19</sup> The Sn catalyst, which exhibits limited stability, is merely used here to demonstrate the utility of the two-phase reactor design and its potential use in the rapid evaluation of other promising catalysts.

The individual electrode polarization curves in Fig. 3c show that the improvements due to lowering the pH are mainly observed on the cathode. In addition to increasing the efficiency for formic acid production, lowering the pH also enhances cathode performance by reducing polarization losses, enabling higher current densities. The use of an external reference electrode in this design enables us to determine that the effects of decreasing pH are on the cathode and not a side effect on the anode performance.

## Conclusions

This study demonstrated a microfluidic electrochemical cell as an effective reactor and a versatile analytical tool for studying the electrochemical reduction of CO<sub>2</sub>. The flowing liquid electrolyte stream employed in this design offers many benefits: (i) wide flexibility in operation conditions, particularly with respect to electrolyte composition and pH; (ii) the electrolyte stream supplies one of the reactants (H<sub>2</sub>O) to the anode and minimizes water management issues at

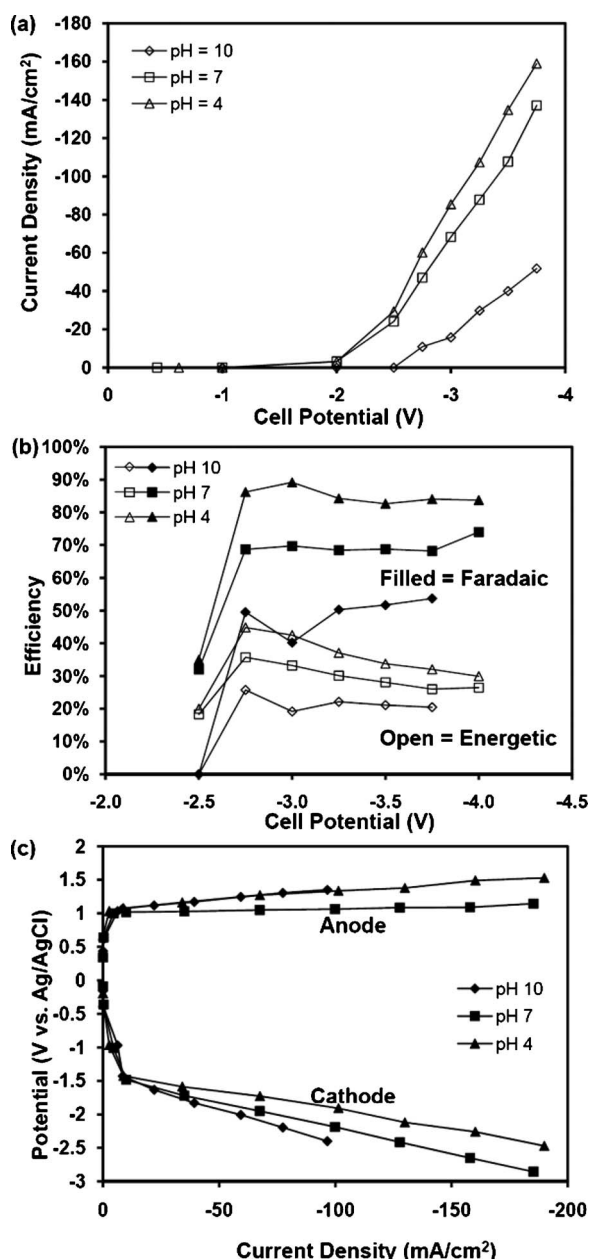


**Figure 3.** (a) Partial current density for a Sn cathode and Pt black anode using 0.5 M KCl adjusted with HCl or KOH to different pH. (b) Faradaic efficiency (filled symbols) and energetic efficiency (open symbols) at different pH. (c) Individual electrode polarization curves for the Sn cathode and Pt anode at different pH.

the electrode surfaces; (iii) a continuous flow operation makes on-line sample collection or product analysis simple and quick; and (iv) the ability to place a reference electrode in the exit steam allows the

analysis of individual electrode performance. We exploited these attractive characteristics to investigate different catalysts and the effects of pH. Furthermore, the cell also serves as an effective reactor with high efficiencies (89% faradaic and 45% energetic) and current densities on the order of 100 mA/cm<sup>2</sup>. Performance could potentially be further improved by engineering of the GDEs at the gas/liquid interface. While the Sn catalyst was used for most of this study, the design is amenable to other catalysts, and the flexibility of this cell can further be used to test other parameters such as temperature and the production of other products such as syngas.

#### Acknowledgments

This work was supported by the National Science Foundation (career grant CTS 05-47617) and the Grainger Center for Electric Machinery and Electromechanics.

*University of Illinois at Urbana-Champaign, assisted in meeting the publication costs of this article.*

#### References

- U.S. EPA, Report no. EPA 430-R-09-004 (2009).
- C. Oloman and H. Li, *ChemSusChem*, **1**, 385 (2008).
- C. M. Sanchez-Sanchez, V. Montiel, D. A. Tryk, A. Aldaz, and A. Fujishima, *Pure Appl. Chem.*, **73**, 1917 (2001).
- M. Azuma, K. Hashimoto, M. Hiramoto, M. Watanabe, and T. Sakata, *J. Electrochem. Soc.*, **137**, 1772 (1990).
- N. Furuya, T. Yamazaki, and M. Shibata, *J. Electroanal. Chem.*, **431**, 39 (1997).
- Y. Hori, H. Wakebe, T. Tsukamoto, and O. Koga, *Electrochim. Acta*, **39**, 1833 (1994).
- M. N. Mahmood, D. Masheder, and C. J. Harty, *J. Appl. Electrochem.*, **17**, 1159 (1987).
- N. Furuya and S. Koide, *Electrochim. Acta*, **36**, 1309 (1991).
- T. Yamamoto, D. A. Tryk, A. Fujishima, and H. Ohata, *Electrochim. Acta*, **47**, 3327 (2002).
- R. L. Cook, R. C. Macduff, and A. F. Sammells, *J. Electrochem. Soc.*, **137**, 607 (1990).
- S. Kaneco, H. Katsumata, T. Suzuki, and K. Ohta, *Energy Fuels*, **20**, 409 (2006).
- G. Arai, T. Harashina, and I. Yasumori, *Chem. Lett.*, **18**, 1215 (1989).
- D. P. Summers, S. Leach, and K. W. Frese, *J. Electroanal. Chem. Interfacial Electrochem.*, **205**, 219 (1986).
- Y. Hori, A. Murata, and R. Takahashi, *J. Chem. Soc., Faraday Trans. 1*, **85**, 2309 (1989).
- H. Li and C. Oloman, *J. Appl. Electrochem.*, **36**, 1105 (2006).
- Y. Akahori, N. Iwanaga, Y. Kato, O. Hamamoto, and M. Ishii, *Electrochemistry (Tokyo, Jpn.)*, **72**, 266 (2004).
- F. Köleli, T. Atılan, N. Palamut, A. M. Gizir, R. Aydin, and C. H. Hamann, *J. Appl. Electrochem.*, **33**, 447 (2003).
- H. Li and C. Oloman, *J. Appl. Electrochem.*, **37**, 1107 (2007).
- K. Subramanian, K. Asokan, D. Jeevarathinam, and M. Chandrasekaran, *J. Appl. Electrochem.*, **37**, 255 (2007).
- B. Innocent, D. Liaigre, D. Pasquier, F. Ropital, J. M. Leger, and K. B. Kokoh, *J. Appl. Electrochem.*, **39**, 227 (2009).
- C. Delacourt, P. L. Ridgway, J. B. Kerr, and J. Newman, *J. Electrochem. Soc.*, **155**, B42 (2008).
- F. Bidrawn, G. Kim, G. Corre, J. T. S. Irvine, J. M. Vohs, and R. J. Gorte, *Electrochem. Solid-State Lett.*, **11**, B167 (2008).
- H. Li and C. Oloman, *J. Appl. Electrochem.*, **35**, 955 (2005).
- R. S. Jayashree, M. Mitchell, D. Natarajan, L. J. Markoski, and P. J. A. Kenis, *Langmuir*, **23**, 6871 (2007).
- R. Sleat and R. A. Mah, *Appl. Environ. Microbiol.*, **47**, 884 (1984).
- A. Deffernez, S. Hermans, and M. Devillers, *Appl. Catal., A*, **282**, 303 (2005).
- R. Larsen, S. Ha, J. Zakzeski, and R. I. Masel, *J. Power Sources*, **157**, 78 (2006).
- F. R. Brushett, W. P. Zhou, R. S. Jayashree, and P. J. A. Kenis, *J. Electrochem. Soc.*, **156**, B565 (2009).
- R. Williams, R. S. Crandall, and A. Bloom, *Appl. Phys. Lett.*, **33**, 381 (1978).
- H. Endo and G. Yokoyama, *Science Reports of the Research Institutes, Tohoku University — Series A: Physics, Chemistry and Metallurgy*, **2**, 449 (1950).